Journal of Photochemistry and Photobiology B: Biology 127 (2013) 1–7

Contents lists available at ScienceDirect

Journal of Photochemistry and Photobiology B: Biology

journal homepage: www.elsevier.com/locate/jphotobiol

Toxic effects of mercury on PSI and PSII activities, membrane potential and transthylakoid proton gradient in *Microsorium pteropus*

Chunnuan Deng [a,b], Daoyong Zhang [b,c], Xiangliang Pan [b,*], Fengqin Chang [a], Shuzhi Wang [b,d]

[a] Key Lab of Plateau Lake Ecology & Global Change, College of Tourism and Geographic Science, Yunnan Provincial Key Laboratory of Plateau Geographical Process and Environmental Change, Yunnan Normal University, Kunming 650500, China
[b] Laboratory of Environmental Pollution and Bioremediation, Xinjiang Institute of Ecology and Geography, Chinese Academy of Sciences, Urumqi 830011, China
[c] State Key Laboratory of Environmental Geochemistry, Institute of Geochemistry, Chinese Academy of Sciences, Guiyang 550002, China
[d] University of Chinese Academy of Sciences, Beijing 100049, China

ARTICLE INFO

Article history:
Received 7 April 2013
Received in revised form 10 July 2013
Accepted 11 July 2013
Available online 20 July 2013

Keywords:
Photosystem I
Mercury
Membrane potential
Proton gradient
Aquatic plant

ABSTRACT

Mercury (Hg) is one of the top toxic metals in environment and it poses a great risk to organisms. This study aimed to elucidate the toxic effects of Hg^{2+} on energy conversion of photosystem I (PSI) and photosystem II (PSII), membrane potential and proton gradient of *Microsorium pteropus* (an aquatic plant species). Contents of chlorophyll *a*, chlorophyll *b* and carotenoids, quantum yield and electron transfer of PSI and PSII of *M. pteropus* exposed to various concentrations of Hg^{2+} were measured. With increasing Hg^{2+} concentration, quantum yield and electron transport of PSI [Y(I) and ETR(I)] and PSII [Y(II) and ETR(II)] decreased whereas limitation of donor side of PSI [Y(ND)] increased. At $\geqslant 165\ \mu g\ L^{-1}$ Hg^{2+}, quantum yield of non-light-induced non-photochemical fluorescence quenching in PSII [Y(NO)] significantly increased but quantum yield of light-induced non-photochemical fluorescence quenching [Y(NPQ)] decreased. Membrane potential ($\Delta\psi$) and proton gradient (ΔpH) of *M. pteropus* were reduced significantly at $330\ \mu g\ L^{-1}$ Hg^{2+} compared to control. Mercury exposure affected multiple sites in PSII and PSI of *M. pteropus*.

1. Introduction

Mercury (Hg) pollution has raised great concern since 1950s with the outbreak of Minamata disease in Japan and has gradually become a problem of environment pollution on global scale [1]. As one of the most toxic metals to human and organisms [2], Hg is known for its non-biodegradability and translocation in the ecosystem and it can lead to some serious biochemical and physiological disorders in plants [3]. Extensive studies show that Hg has toxicity to photosynthetic apparatus of higher plants, cyanobacteria and algae [3–5]. Many sites in the photosynthetic membrane, especially the photosystem II (PSII), are highly sensitive to Hg. Mercury can bind strongly to the thiol groups in proteins in both the donor and the acceptor sides of PSII and consequently disturbs their functions [6]. For example, mercury acts on the donor side of PSII by perturbing chloride binding and damaging the oxygen evolving complex [4]. On the acceptor side, the fraction of closed reaction centers increases and the electron transfer from Q_A and Q_B is thus inhibited under Hg stress [7]. Hg affects activities of both PSII and PSI and decreases the whole chian electron transport activities [8,9]. Photosynthetic pigment synthesis, metabolic activity of PSII and cell membranes can be negatively affected by Hg [2,10,11]. After exposure to Hg stress, the proportion of the Q_B-non-reducing PSII reaction centers increases significantly whereas the maximal PSII photochemical efficiency and the quantum yield of PSII electron transport decrease [9,12,13]. Hg can also lead to an increase of high energy state quenching [14] as well as inhibition of excitation energy transfer from phycobilisomes to PSII reaction centers [15]. Photosystem I (PSI) reaction centers could be damaged [16] and the PSI activity could be reduced under stress of Hg [4]. Murthy and Mohanty reported that Hg^{2+} inhibited the whole chain electron transport in PSI and PSII even at low concentration by damaging the intersystem electron transport carriers [5]. Some studies show that PSI is less affected than PSII under Hg stress [8,9], suggesting that PSI is not a controlling factor in total photosynthesis activity [4]. Therefore, toxic effects of Hg on function and regulation mechanism of PSI and PSII need further study.

In photosynthesis process, free energy released from exergonic reaction is stored in the form of transmembrane electrochemical gradient of protons, i.e., proton motive force (pmf) [17]. The pmf is coupled to ATP synthesis and composed of the transmembrane differences in the proton concentration (proton gradient, ΔpH)

* Corresponding author. Address: Laboratory of Environmental Pollution and Bioremediation, State Key Laboratory of Desert and Oasis Ecology, Xinjiang Institute of Ecology and Geography, Chinese Academy of Sciences, Urumqi 830011, China. Tel./fax: +86 991 7885446.
E-mail address: xlpan@ms.xjb.ac.cn (X. Pan).

1011-1344/$ - see front matter © 2013 Elsevier B.V. All rights reserved.
http://dx.doi.org/10.1016/j.jphotobiol.2013.07.012

and the electric field (membrane potential, $\Delta\psi$) [17]. ΔpH and $\Delta\psi$ carry fundamental information on the rates of coupled electron and proton transport [18]. ΔpH affects the turnover rates of key photosynthetic enzymes and initiates downregulatory processes [17]. The light-dependent H^+ partitioning between thylakoids and stroma controls the rate of plastoquinol oxidation at $Cytb_6f$ [19]. The formation of ΔpH is closely correlated with the non-photochemical fluorescence quenching [20,21]. The photogenerated $\Delta\psi$ drives fluxes of divalent cations that modulate enzyme activities in the chloroplast stroma [22]. $\Delta\psi$ influences electrogenic reactions in PSII, PSI and $Cytb_6f$ complex [23]. Wang et al. reported that the build-up of ΔpH of mutant tobacco was significantly inhibited under high tempreture (42°C) stress [24]. Regardless of their important function in the photosynthesis, responses of membrane potential ($\Delta\psi$) and proton gradient (ΔpH) to environmental stresses have been limitedly investigated [17,22,25].

The Dual-PAM-100 system produced by WALZ (Walz, Germany) can simultaneously *in vivo* record PSI and PSII activities. Recently, the Dual-PAM-100 system has been demonstrated to be a powerful tool for probing responses and regulation mechanism of PSI and PSII under environmental stresses [26–29]. Besides measuring P700 and chlorophyll (Chl) fluorescence, the system can be extended by optional emitter-detector modules for assessment of P515 signal to analyze transthylakoid proton gradient (ΔpH) and membrane potential ($\Delta\psi$) [18]. In the present study, effects of mercury on the energy conversion and electron transport in PSI and PSII, membrane potential ($\Delta\psi$) and proton gradient (ΔpH) of *Microsorium pteropus*, a common aquatic fern, were investigated.

2. Materials and methods

2.1. Plant materials and mercury treatment

M. pteropus seedlings about 25 cm height were purchased from the market and cultured in tap water at 25 °C and 100 μmol photons m^{-2} s^{-1} with a 12: 12 h light: dark photoperiod. After one week of acclimation, the plants were transferred to 1 L of tap water containing various concentrations of mercury (0–330 μg L^{-1}). Mercury ($HgCl_2$) was dissolved in tap water and diluted to the desired concentrations. The samples without addition of mercury were used as control. After 3 days of treatment, PSI and PSII activities, membrane potential and proton gradient, and content of pigments were measured.

2.2. Measurement of pigments content

About 0.2 g of *M. pteropus* fresh leaves was homogenized and then extracted with 80% acetone for 24 h at 4 °C in the dark. Absorption of the extracted pigment solution was measured at 663, 645 and 470 nm with a spectrophotometer (UV2800, Unico, Shanghai, China). Contents of Chl *a*, Chl *b* and carotenoids were calculated according to Lichtenthaler and Wellburn [31].

2.3. Measurement of energy conversion in PSI and PSII

PSI and PSII activities of *M. pteropus* leaves were measured simultaneously using a Dual-PAM-100 system (Heinz Walz GmbH, Effeltrich, Germany). All samples were dark-adapted for 5 min prior to measurement. Measurement was carried out using the automated program of the Dual-PAM software [32]. The minimal fluorescence (F_0) was determined by measuring light. A saturating pulse with a 300 ms 10,000 μmol photons m^{-2} s^{-1} light was applied to determine the maximum fluorescence (F_m). The maximal change in P700 signal (P_m) was measured through the application of a saturation pulse after far-red pre-illumination for 10 s according to the method of Klughammer and Schreiber [33].

After determination of F_0, F_m and P_m, the slow induction curve was recorded with the routine program of the Dual-PAM-100 software. An actinic light at 30 μmol m^{-2} s^{-1} was applied. A saturating pulse with duration of 300 ms was applied every 20 s after the onset of the actinic light to determine the maximum fluorescence signal (F'_m) and maximum $P700^+$ signal (P'_m) under the actinic light. The slow induction curve was recorded for 120 s to achieve the steady state of the photosynthetic apparatus, and then the actinic light was turned off. The P700 signal (P) was recorded just before a saturation pulse then briefly after onset of a saturation pulse (F'_m), when the maximum P700 oxidation was observed. Finally, P_0 was determined at the end of the 1 s dark interval following each saturation pulse. The signals P and F'_m were detected referencing against P_0.

The quantum yields of PSI and PSII were measured by saturating pulses during the process of slow induction curve and calculated automatically by the Dual-PAM-100 software according to the method of Klughammer and Schreiber [33] and Kramer et al. [34]: $Y(II) = (F'_m - F)/F'_m$, $Y(NPQ) = F/F'_m - F/F_m$, $Y(NO) = F/F_m$ [where F was the steady state fluorescence, Y(II) was the effective photochemical quantum yield of PSII, Y(NPQ) was the quantum yield of light-induced non-photochemical fluorescence quenching, and Y(NO) was the quantum yield of non-light-induced non-photochemical fluorescence quenching]; $Y(I) = (P'_m - P)/P_m$, $Y(ND) = (P - P_0)/P_m$, $Y(NA) = (P_m - P'_m)/P_m$ [where Y(I) was effective photochemical quantum yield of PSI, Y(ND) was the quantum yield of non-photochemical energy dissipation in reaction centers due to PSI donor side limitation, and Y(NA) was the quantum yield of non-photochemical energy dissipation of reaction centers due to PSI acceptor side limitation].

2.4. Electron transport in PSI and PSII

Electron transport rates (ETRs) in PSI and PSII, i.e., ETR(I) and ETR(II), were recorded during the measurement of the slow induction curve. They were defined and calculated using the Dual-PAM software as $ETR(I) = Y(I) \times PAR \times 0.84 \times 0.5$ and $ETR(II) = Y(II) \times PAR \times 0.84 \times 0.5$ [35]. The response of the activities of electron transport in PSI and PSII to increasing irradiation were further measured as rapid light curves (RLCs). The rapid light curve consists of the electron transport responses to eleven irradiances (PAR 0, 11, 18, 27, 42, 58, 100, 221, 344, 536 and 830 μmol photons m^{-2} s^{-1}) for 30 s with increasing intensity. Important parameters of ETR(I) and ETR(II) in light response reaction were derived from the RLCs, which were automatically calculated by the Dual-PAM software according to the exponential function referring to Platt et al. [36]. The parameters calculated were as follows: α, the initial slope of RLC of ETR(I) or ETR(II), which reflected the quantum yield [37] of PSI or PSII; ETR_{max}, the maximal electron transport rates in PSI or PSII; I_k, the index of light adaptation of PSI or PSII (i.e., determined from the interception point of the alpha value with the maximum photosynthetic rate), was calculated as ETR_{max}/α [36].

2.5. Measurement of membrane potential($\Delta\psi$) and proton gradient (ΔpH)

Transthylakoid proton gradient (ΔpH) and membrane potential ($\Delta\psi$) can be measured automatically through extended emitter-detector modules as P515/535 [18] with the Dual-PAM-100 system. The P515/535 module consists of the emitter unit DUAL-EP515 and the detector unit DUAL-DP515, optical design and outer appearance of which are equivalent to the standard emitter detector units for simultaneous measurement of P700 and Chl fluorescence [18]. After longer dark times are given, the P515 displays complex relaxation kinetics for differentiation between $\Delta\psi$ and ΔpH components of the overall proton motive force (pmf) [17]. According to Kramer and Co-workers [38] the relative amplitudes of $\Delta\psi$ and ΔpH can

be estimated from the characteristic levels observed during the light-off response. The difference between the steady state signal and the "dark baseline" reflects $\Delta\psi$ during steady state illumination. The "undershoot" below the "dark baseline" is considered to be a measurement of the steady state of ΔpH. When light is off the accumulated protons are rapidly released from the lumen to the stroma via the ATP-ase, and there is a sudden excess of negative charge at the internal side of the membrane, which results in an inversed P515. The 550–515 nm signal reflects P515 and zeaxanthin change as well. The dark-light and light-dark induced 550–515 nm changes in the sub-s to min time range are almost exclusively due to P515, whereas the slower changes ranging from minutes to hours reflect zeaxanthin formation and zeaxanthin epoxidation, respectively. Before measurement, plant samples were kept for 30 min in darkness. The original difference of signals were measured in Volt units, which were transformed into $\Delta I/I$ units with the help of the calibration routine. The 550–515 nm signal curves were recorded at dark-light (120 s) – dark cycle by the Dual-PAM-100 software. $\Delta\psi$ and ΔpH components of the overall proton motive force (pmf) were calculated in $\Delta I/I$ units [18].

2.6. Statistics

Each treatment was replicated three times. Means and standard deviations (S.D.) were calculated. The statistical significance between treatments and control were performed by one-way ANOVA (SPSS V16.0) through the least significant difference (LSD) test.

3. Results

3.1. Hg uptake in plants

Hg^{2+} was efficiently uptaken by *M. pteropus* after the plants were exposed to various concentrations of Hg^{2+} for 3 days. Hg^{2+} concentration in plant tissues increased significantly with increasing Hg^{2+} concentration (Fig. 1, $P < 0.001$). Hg^{2+} content in plants was 3.4 mg kg^{-1} DW at 3.3 μg L^{-1} Hg^{2+} and 212.5 mg kg^{-1} DW at 330 μg L^{-1} Hg^{2+}.

3.2. Effects on content of pigments

Hg^{2+} at 3.3 μg L^{-1} reduced Chl *a*, Chl *b* and carotenoids contents of *M. pteropus* compared with control in marginal significance. Hg^{2+} at 33 μg L^{-1} or higher concentrations significantly reduced content of all the pigments with respect to the control (Fig. 2). Chl *a* decreased from 0.296 g kg^{-1} FW for control to 0.204 g kg^{-1} FW at 330 μg L^{-1} Hg^{2+}. Chl *b* decreased by 30% at 330 μg L^{-1} Hg^{2+} in comparison with the control. Carotenoids content decreased from 0.719 g kg^{-1} FW for control to 0.474 g kg^{-1} FW at 330 μg L^{-1} Hg^{2+}. Chl *a*, Chl *b* and carotenoids under Hg^{2+} exposure decreased significantly but there is no significant difference between samples treated with various concentrations of Hg^{2+}.

3.3. Effects on energy conversion of PSI and PSII

Energy conversion of PSI and PSII were significantly influenced after 3 days of Hg^{2+} treatment (Fig. 3A and B). Y(I) (quantum yield of PSI) decreased with increasing Hg^{2+} concentration from 3.3 to 330 μg L^{-1} accompanied with the increase of Y(ND) (PSI donor side limitation). Y(I) decreased by 19%, while Y(ND) increased by 32% at 3.3 μg L^{-1} Hg^{2+} compared with the control. The value of PSI acceptor side limitation [Y(NA)] did not change significantly at various concentrations of Hg^{2+} compared with the control (Fig. 3A). Data of Y(I), Y(ND) and Y(NA) at 330 μg L^{-1} Hg^{2+} were not shown because the data were not reliably measured due to their significant fluctuation at higher Hg^{2+} concentration. Y(II) (quantum yield of PSII) significantly decreased as Hg^{2+} concentration increased, associated with an increase of Y(NO) (quantum yield of non-light-induced non-photochemical fluorescence quenching). At 3.3 μg L^{-1} Hg^{2+}, Y(II) decreased by 30% whereas Y(ND) and Y(NPQ) (quantum yield of light-induced non-photochemical fluorescence quenching) increased by 1% and 83% respectively compared to the control. In comparison with the control, Y(NPQ) increased at 3.3–165 μg L^{-1} Hg^{2+} and decreased at 330 μg L^{-1} Hg^{2+} (Fig. 3B).

3.4. Electron transport of PSI and PSII

Both ETR_{max}(I) and ETR_{max}(II) significantly decreased with increasing Hg^{2+} concentration (Fig. 4A and B and Table 1). Compared to the control, ETR_{max}(I) and ETR_{max}(II) decreased by 35% and 55% at 3.3 μg L^{-1} Hg^{2+} and decreased by 55% and 67% at 165 μg L^{-1} Hg^{2+}, respectively. Compared with the control, the values of I_k(I) and I_k(II) also markedly decreased at various concentrations of Hg^{2+}. I_k(I) and I_k(II) decreased by 56% and 65% at 165 μg L^{-1} Hg^{2+}, respectively compared to control. The values of *a*(II) and

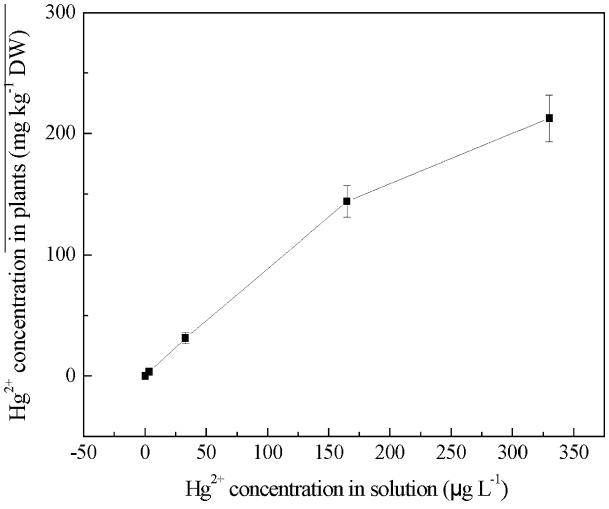

Fig. 1. Hg^{2+} content (mg kg^{-1} DW) in plants grown in solution containing various concentrations of Hg^{2+} (μg L^{-1}). Each treatment was triplicated. Error bars represented standard errors.

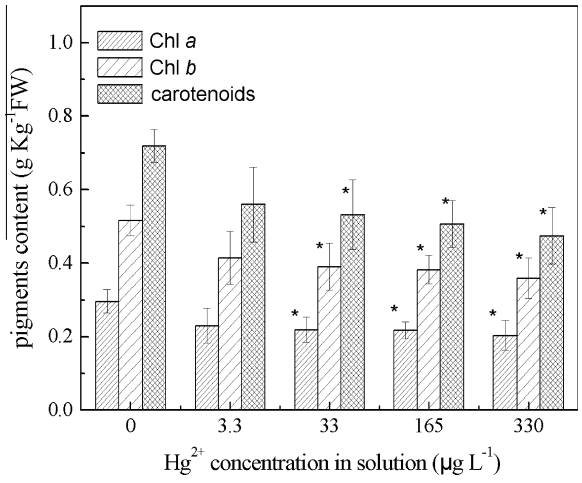

Fig. 2. Content of Chl *a*, Chl *b* and carotenoids of *M. pteropus* treated with various concentrations of Hg^{2+} for 3 days ($n = 3$) (significant levels between control and treatment groups were indicated by asterisks, $^{*}p < 0.05$).

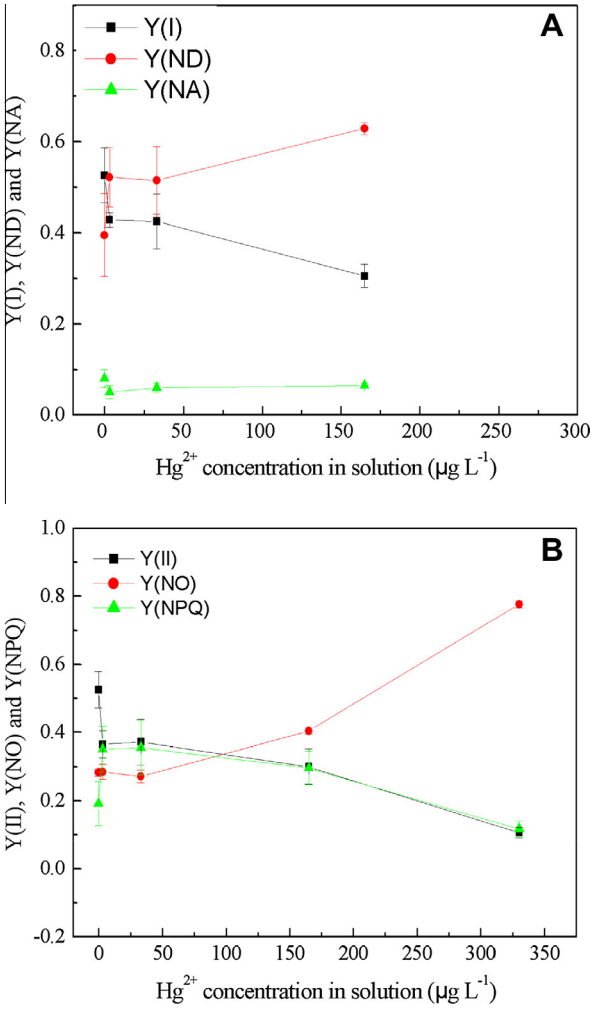

Fig. 3. Y(I), Y(ND) and Y(NA) of PSI (Fig. 3A), and Y(II), Y(NO) and Y(NPQ) of PSII (Fig. 3B) of *M. pteropus* exposed to various concentrations of Hg^{2+} for 3 days. All data presented were mean values of three duplications (Data of Y(I), Y(ND) and Y(NA) at 330 μg L^{-1} Hg^{2+} were not shown in Fig. 3A because the data were not reliably measured due to their significant fluctulation).

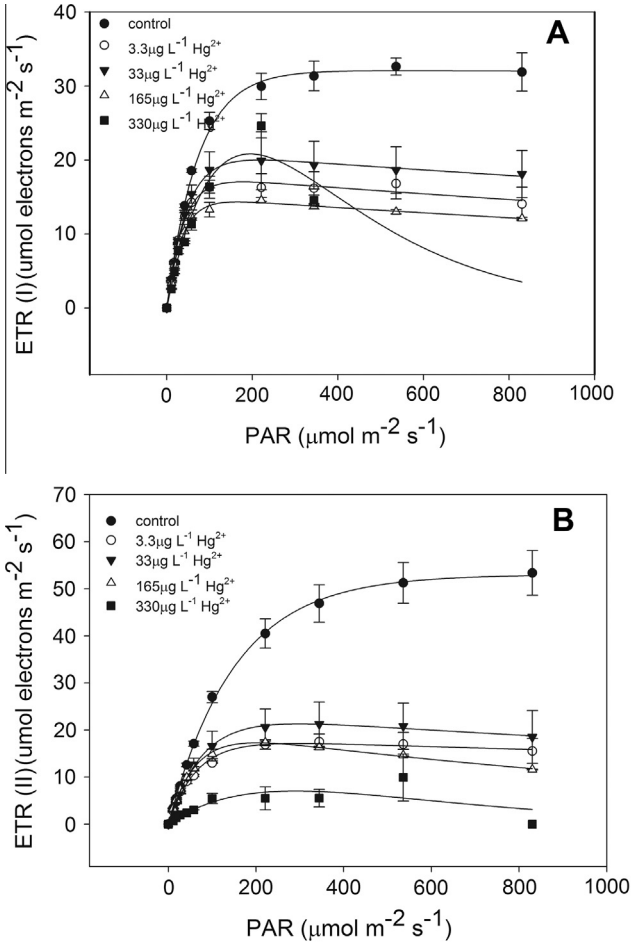

Fig. 4. The rapid light curves (RLCs) of ETR(I) (Fig. 4A) and the RLCs of ETR(II) (Fig. 4B). Data were detected through the light response reaction after 3 days of exposure to various concentrations of Hg^{2+}. The RLCs of ETR(I) and ETR(II) were recorded by the Dual-PAM system during the light response reaction, where PAR increased from 0 to 830 μmol photons m^{-2} s^{-1}. All the data presented here were calculated from three duplication.

a(I) changed slightly at various concentration of Hg^{2+} in comparison with the control (Table 1).

3.5. Change of membrane potential($\Delta\psi$) and proton gradient(ΔpH) under Hg^{2+} stress

$\Delta\psi$ and ΔpH generally decreased with the increase of Hg^{2+} concentration ($p < 0.05$ at 330 μg L^{-1} Hg^{2+}) (Fig. 5A and B). $\Delta\psi$ decreased by 47% from 11.536 $\Delta I/I \times 10^{-3}$ for control to 6.060 $\Delta I/I \times 10^{-3}$ at 330 μg L^{-1} Hg^{2+}. ΔpH decreased by 64% from 5.192 $\Delta I/I \times 10^{-3}$ for control to 1.881 $\Delta I/I \times 10^{-3}$ at 330 μg L^{-1} Hg^{2+}.

4. Discussion

In the present study, effects of Hg^{2+} on pigments concentration, energy conversion and electron transport of PSI and PSII, membrane potential and proton gradient in *M. pteropus* were analyzed.

Chl *a*, Chl *b* and carotenoids content decreased with increasing Hg^{2+} concentration, which is in consistent with previous studies [10,39], suggesting that Chl *a*, Chl *b* and carotenoids synthesis were influenced significantly under mercury stress, chlorophyll pigments seem to be one of the sites of mercury injury. Loss of light harvesting pigments due to heavy metal treatment has been reported in higher plants and cyanobacteria [2,30,40]. The decrease of Chl *a* content after exposure to Hg^{2+} stress may be due to the replacement of Mg^{2+} by Hg^{2+} in chlorophyll molecules [41] or the inhibition of chlorophyll synthesis [10,42], which consequently leads to a reduction of photosynthesis. Because about 90% of the total Chl *b* is bound to LHCII (light-harvesting chlorophyll *a*/*b* – protein complex of PSII), decrease of Chl *b* indicates the degradation of LHCII [43]. Under heavy metal stress, Chl *b* usually increases because of the transformation of Chl *a* to Chl *b* [44]. However, sometimes mercury exposure decreased Chl *b* content [10,45,46]. The results of the present study was in consistent with the latter, which at least implies that transformation of Chl *a* to Chl *b* was not noticeable. There was no significant difference between the effects of 33 and 330 μg L^{-1} Hg^{2+} on the content of Chl *a*, *b* and carotenoids (Fig. 2). The possible reason maybe that Hg^{2+} ions only replaced part of the Mg^{2+} and 3.3 μg L^{-1} Hg^{2+} are enough to substitute the Mg^{2+} that can be replaced. Similarly, 3.3 μg L^{-1} Hg^{2+} are enough to exert full action on synthesis of Chl *b* and carotenoids. In other words, Hg^{2+} above 3.3 μg L^{-1} Hg^{2+} could not exert more inhibitory effect on synthesis of Chl *b* and carotenoids. Carotenoids plays a special role in the thermal dissipation of excess light energy [47]. Depletion of carotenoids will decrease the primary photochemistry and photosynthetic oxygen evolution and affect the PSI photochemistry [47]. The inhibition of synthesis

Table 1
Parameters of electron transport of PSII and PSI derived from the rapid light curves (RLCs) of ETR(II) and ETR(I) according to Platt et al. [36].

Hg^{2+} concentration ($\mu g\ L^{-1}$)	Parameters of RLCs of ETR(I)			Parameters of RLCs of ETR(II)		
	A (e^- photon^{-1})	ETR_{max} ($\mu mol\ e^-\ m^{-2}\ s^{-1}$)	I_k (μmol photon $m^{-2}\ s^{-1}$)	α (e^- photon^{-1})	ETR_{max} ($\mu mol\ e^-\ m^{-2}\ s^{-1}$)	I_k (μmol photon $m^{-2}\ s^{-1}$)
0	0.443 ± 0.004	32.10 ± 2.828	72.55 ± 7.142	0.352 ± 0.017	53.00 ± 7.071	150.30 ± 13.011
3.3	0.449 ± 0.037	21.03 ± 7.032*	47.77 ± 10.321	0.297 ± 0.030	24.00 ± 5.784*	78.99 ± 19.320*
33	0.459 ± 0.037	20.10 ± 3.775*	44.33 ± 8.740	0.308 ± 0.023	21.467 ± 5.547*	69.50 ± 15.734*
165	0.458 ± 0.038	14.60 ± 4.313*	31.90 ± 4.950*	0.328 ± 0.020	17.30 ± 0.283*	52.70 ± 2.616*
330	–**	–**	–**	–**	–**	–**

* $p < 0.05$.
** Because ETR(I) at 330 $\mu g\ L^{-1}$ Hg^{2+} fluctuated signifcantly and ETR(II) were very low and their derived parameters could not be reliably calculated, these parameters were not given in Table 1.

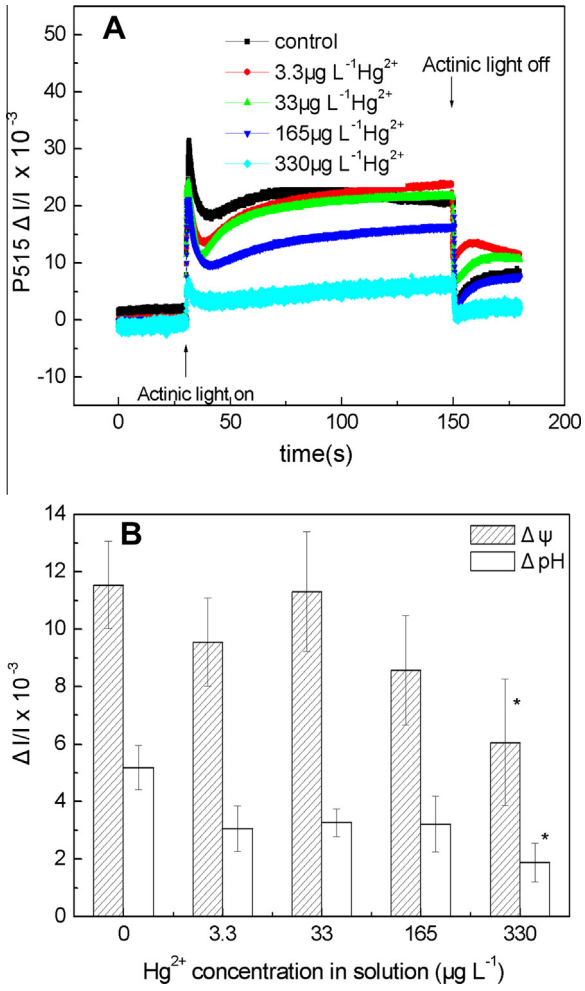

Fig. 5. (A) Effect of Hg^{2+} on P515 signals. P515 signals were measured as described in Section 2. At 30 s, samples were illuminated with 126 $\mu mol\ m^{-2}\ s^{-1}$ of photons of red light for 120 s. After 120 s of actinic light illumination, samples were relaxed in the dark for 30 s. (B) Effect of Hg^{2+} on membrane potential ($\Delta\psi$) and proton gradient (ΔpH) components of the overall proton motive force (pmf), calculated from the curves of P515 signals.

of carotenoids under Hg^{2+} stress caused the block of the dissipation of harmful excess excitation energy [48], i.e., the decrease of Y(NPQ) (Fig. 3B). The inhibition of synthesis of pigments causes the decrease of photosynthetic activity in the present study.

Mercury exerts its action on many sites in the photosynthetic membrane. PSII is the most sensitive target including its donor and acceptor sides [49,50]. Lu et al. reported that an increase in Hg^{2+} concentration led to a decrease in quantum yield of PSII [51]. Singh et al. reported that mercury inhibited PSII activity of cyanobacterium *Nostoc muscorum* [9]. Hg-induced toxicity results from binding of its ionic form (Hg^{2+}) to sulphydryl groups of proteins, disruption of structure and displacement of essential elements [52,53]. Inhibition of PSII activity has been ascribed to the loss of D1 protein [54] and degradation of pigment content. Compared to PSII, PSI is reported to be less sensitive to stresses because of its greater stability and lesser abundance in thylakoid membrane [9,55]. In the present study, mercury inhibited PSII more than PSI. Inhibition of PSII was accompanied by an increase of Y(NO) and a decrease of Y(NPQ) for Hg^{2+} treated samples compared with control (Fig. 3B). Y(NPQ) represents excess PSII energy that could be dissipated via regulated mechanism concerning xanthophyll cycle and carotenoids. The increase of Y(NPQ) at low and middle levels of Hg^{2+} means that excessive excitation energy could be efficiently dissipated into harmless heat, while the decrease of Y(NPQ) at $\geqslant$165 $\mu g\ L^{-1}$ Hg^{2+} suggests that regulation mechanism of energy does not work well at $\geqslant$165 $\mu g\ L^{-1}$ Hg^{2+} [35]. Y(NO) represents excess PSII energy that should be dissipated via non-regulated processes [34]. The increase of Y(NO) reflects the increase of fraction of closed PSII centers [33], and the failure of reaction centers to cope with the excess radiation [33] at high levels of Hg^{2+}.

In the present study, Hg^{2+} significantly inhibited the activity of PSI. PSI is important for cyclic electron flow, which generates a transthylakoid H^+ gradient (ΔpH) for ATP synthesis. The decrease of Y(I) indicates a significant obstacle to effective photosynthetic function [56]. The simultaneous decrease of Y(I) and Y(II) suggests that electron transport of PSII and PSI were inhibited by Hg^{2+}. The decreases of ETR_{max} (II) and ETR_{max} (I) (Fig. 4A and B and Table 1) and increase of Y(ND) (Fig. 3A) confirmed this inhibitory effect. The significant increase of Y(ND) and little change of Y(NA) implies that the decrease of quantum yield of PSI was mainly due to the limitation of donor side of PSI. Y(ND) is the fraction of oxidized P700 due to a lack of donors or deprivation of electrons of PSI [57]. Small antenna size in PSII can efficiently restrict PSI photochemistry via donor side limitation through inefficient light absorption [32]. The significant increase of Y(ND) at $\leqslant$165 $\mu g\ L^{-1}$ Hg^{2+} indicates that PSI in *M. pteropus* is still physiologically healthy and well-regulated [18], and the restricted photochemistry of PSI is owing to inefficient light absorption in PSII. At 330 $\mu g\ L^{-1}$ Hg^{2+}, the PSI became unstable and no reliable data of Y(I), Y(ND) and Y(NA) were measured, suggesting that high levels of Hg^{2+} damaged the function of PSI. The decreased I_k(II) and I_k(I) for Hg^{2+} treated plants showed that mercury toxicity triggered photoinhibition. The threshold of irradiance that plant can tolerate decreased and photodamage will occur at lower light intensities [58], which was reported on pea leaves under heavy metal stress [59].

According to the Mitchell's chemiosmotic theory, the intermediate that couples the electron flow through the respiratory chain with ATP synthesis by ATP synthase in the mitochondrial matrix

is the proton motive force across the inner mitochondrial membrane. P515 signals carry fundamental information on the rates of coupled electron and proton transport, and reflect H^+ efflux from the lumen to the stroma via thylakoid ATP-ase. According to Mitchell's chemiosmotic hypothesis, the proton motive force can be parsed into the transmembrane proton gradient (ΔpH) and the electric field gradient ($\Delta\psi$), which is thermodynamically equivalent [60]. The ATP/ADP carrier is driven by $\Delta\psi$, whereas the phosphate carrier is driven by ΔpH [61]. Under dark-light-dark induction, an increase of P515 signals reflects not only an increase of the membrane potential but also the formation of zeaxanthin, which is reflected by ΔpH. NPQ is mainly associated with the transthylakoid proton gradient (ΔpH) and xanthophyll cycle [62]. The ΔpH component is the key regulatory signal for initiation of non-photochemical quenching (NPQ) of excitation energy [63]. In the present study, meHHembrane potential ($\Delta\psi$) and proton gradient (ΔpH) components of *M. pteropus* decreased with the increase of Hg^{2+} concentration, suggesting that the formation of zeaxanthin was inhibited, H^+ efflux from the lumen to the stroma via thylakoid ATP-ase was reduced, and the non-photochemical quenching mechanism was impaired at high levels of Hg^{2+}. Antal et al. reported that in the presence of valinomycin, the transthylakoid membrane potential ($\Delta\psi$) was significantly inhibited [23]. Some other environmental stresses could also decrease the membrane potential and proton gradient [23,24,64]. A decrease of either ΔpH or $\Delta\psi$ can reduce the photosynthetic rate of *Chlamydomonas reinhardtii*, with more contribution of ΔpH to the photosynthesis [65]. The present study showed that ΔpH decreased more than $\Delta\psi$ under mercury exposure, suggesting that NPQ were seriously inhibited while ATP driver was less affected.

In the present study, Chl *a*, Chl *b* and carotenoids contents decreased with the increase of Hg^{2+} concentration. Quantum yield of PSI and PSII significantly decreased under Hg^{2+} stress. The decrease of Y(I) is mainly caused by the limitation of Y(ND). The severe damage of PSII at high levels of Hg^{2+} is due to the failure of regulation mechanism of energy and dissipation of the excessive excitation energy into harmless heat. The significant decrease of $\Delta\psi$ and ΔpH at 330 μg L^{-1} Hg^{2+} indicates that the formation of zeaxanthin and H^+ efflux from the lumen to the stroma via thylakoid ATP-ase are inhibited, and the non-photochemical quenching mechanism is impaired.

5. Abbreviations

ADP	adenosine diphosphate
ATP	adenosine triphosphate
Chl	chlorophyll
ETR	electron transport rate
ETR(I)	electron transport rates (ETRs) in PSI
ETR(II)	electron transport rates (ETRs) in PSII
ETR_{max}	the maximal electron transport rates in PSI or PSII
I_k	the index of light adaptation of PSI or PSII
LHCII	light-harvesting chlorophylla/b-protein complex of photosystem II
NPQ	non-photochemical quenching
PAR	photosynthetically active radiation
pmf	proton motive force
PSI	photosystem I
PSII	photosystem II
RLC	rapid light curve
Y(I)	the effective photochemical quantum yield of PSI
Y(II)	the effective photochemical quantum yield of PSII
Y(NA)	the quantum yield of non-photochemical energy dissipation of reaction centers due to PSI acceptor side limitation
Y(ND)	the quantum yield of non-photochemical energy dissipation in reaction centers due to PSI donor side limitation
Y(NO)	the quantum yield of non-light-induced non-photochemical fluorescence quenching
Y(NPQ)	the quantum yield of light-induced non-photochemical fluorescence quenching
α	the initial slope of RLC of ETR(I) or ETR(II)
ΔpH	proton gradient
$\Delta\psi$	membrane potential

Acknowledgements

This work was supported by Program of 100 Distinguished Young Scientists of the Chinese Academy of Sciences and National Natural Science Foundations of China (U1120302, 21177127 and 4090300D0301).

References

[1] M. Patra, A. Sharma, Mercury toxicity in plants, Bot. Rev. 66 (2000) 379–422.
[2] V. Nicolardi, G. Cai, L. Parrotta, M. Puglia, L. Bianchi, L. Bini, C. Gaggi, The adaptive response of lichens to mercury exposure involves changes in the photosynthetic machinery, Environ. Pollut. 160 (2012) 1–10.
[3] E. Asztalos, G. Sipka, M. Kis, M. Trotta, P. Maroti, The reaction center is the sensitive target of the mercury(II) ion in intact cells of photosynthetic bacteria, Photosynth. Res. 112 (2012) 129–140.
[4] L.F. De Filippis, R. Hampp, H. Ziegler, The effects of sublethal concentrations of zinc, cadmium and mercury on euglena II. Respiration, photosynthesis and photochemical activities, Arch. Microbiol. 128 (1981) 407–411.
[5] S.D.S. Murthy, P. Mohanty, Mercury ions inhibit photosynthetic electron transport at multiple sites in the cyanobacterium Synechococcus 6301, J. Biosci. 18 (1993) 355–360.
[6] M. Patra, N. Bhowmik, B. Bandopadhyay, A. Sharma, Comparison of mercuy, lead and arsenic with respect to genotoxic effects on plant systems and the development of genetic tolerance, Environ. Exp. Bot. 52 (2004) 199–223.
[7] G.L. Kukarskikh, E.E. Graevskaia, T.E. Krendeleva, K.N. Timofeedv, A.B. Rubn, Effect of methylmercury on primary photosynthesis processes in green microalgae *Chlamydomonas reinhardtii*, Biofizika 48 (2003) 853–859.
[8] H. Clijsters, F. Van Assche, Inhibition of photosynthesis by heavy metal, Photosynth. Res. 7 (1985) 31–40.
[9] R. Singh, G. Dubey, V.P. Singh, P.K. Srivastava, S. Kumar, S.M. Prasad, High light intensity augments mercury toxicity in cyanobacterium *Nostoc muscorum*, Biol. Trace Elem. Res. 149 (2012) 262–272.
[10] T. Pisani, S. Munzi, L. Paoli, M. Bačkor, J. Kováčik, J. Piovár, S. Lppi, Physiological effects of mercury in the liches *Cladonia arbuscula* subsp. *mitis*(Sandst.) Ruoss and *Peltigera rufescens* (Weiss) Humb., Chemosphere 82 (2011) 1030–1037.
[11] S.D.S. Murthy, N. Mohanty, P. Mohanty, Prolonged incubation of mercury alters energy transfer and chlorophyll (Chl) a protein complexes in Synechococcus 6301: change in Chl a absorption and emission characteristics and loss of the F695 emission band, Biometals 8 (1995) 237–242.
[12] G. Samson, R. Popovic, Inhibitory effects of mercury on photosystem II photochemistry in *Dunaliella tertiolecta* under *in vivo* conditions, J. Photochem. Photobiol. B: Biol. 5 (1990) 303–310.
[13] P. Juneau, D. Dewez, S. Matsui, S.G. Kim, R. Popovic, Evaluation of different algal species sensitivity to mercury and metolachlor by PAM-fluorometry, Chemosphere 45 (2001) 589.
[14] D.P. Singh, P. Khare, P.S. Bisen, Effects of Ni^{2+}, Hg^{2+} and Cu^{2+} on growth, oxygen evolution and photosynthetic electron transport in *Cylindrospermum* IU 942, J. Plant Physiol. 134 (1989) 406–412.
[15] S.D.S. Murthy, S.C. Sabat, P. Mohanty, Mercury-induced inhibition of photosystem II activity and changes in the emission of fluorescence from phycobilisoms in intact cells of the cyanobacterium, *Spirulina platensis*, Plant Cell Physiol. 30 (1989) 1153–1157.
[16] Y. Kojima, T. Hiyama, H. Sakurai, Effect of mercurials on iron sulfur centers of PSI of *Anacystis nidulans*, in: J. Biggins (Ed.), Progress in Photosynthesis Research, Nijhoff/Junk, The Hague, 1987, pp. 57–60.
[17] J.A. Cruz, C.A. Sacksteder, A. Kanazawa, D.M. Kramer, Contribution of electric field ($\Delta\psi$) to steady-state transtrylakoid proton motive force (pmf) in Vitro and in Vivo. Control of pmf parsing into $\Delta\psi$ and ΔpH by Ionic strength, Biochemistry 40 (2001) 1226–1237.

[18] U. Schreiber, C. Klughammer, New accessory for the Dual-PAM-100: the P515/535 module and examples of its application, PAM Appl. Notes 1 (2008) 1–10.
[19] N.R. Baker, J. Harbinson, D.M. Kramer, Determining the limitations and regulation of photosynthetic energy transduction in leaves, Plant Cell Environ. 30 (2007) 1107–1125.
[20] W. Bilger, O. Björkman, S.S. Thayer, Light-induced spectral absorbance changes in relation to photosynthesis and the epoxidation state of xanthophyll cycle components in cotton leaves, Plant Physiol. 91 (1989) 542–551.
[21] M.P. Johnson, A.V. Ruban, Rethinking the existence of a steady-state $\Delta\varphi$ component of the proton motive force across plant thylakoid membranes, Photosynth. Res. (2013), http://dx.doi.org/10.1007/s11120-013-9817-2.
[22] A.A. Bulychev, V.A. Osipov, D.N. Matorin, W.J. Vredenberg, Effects of far-red light on fluorescence induction in infiltrated pea leaves under diminished ΔpH and $\Delta\varphi$ components of the proton motive force, J. Bioenergy Biomembr. 45 (2013) 37–45.
[23] T.K. Antal, V. Osipov, D.N. Matorin, A.B. Rubin, Membrane potential is involed in regulation of photosynthetic reactions in the marine diatom *Thalassiosira weissflogii*, J. Photochem. Photobiol. B: Biol. 102 (2011) 169–173.
[24] P. Wang, J.Y. Ye, Y.G. Shen, H.L. Mi, The role of chloroplast NAD(P)H dehydrogenase in protection of tobacco plant against heat stress, Sci China Life Sci. 49 (2006) 311–321.
[25] R. Zhang, T.D. Sharkey, Photosynthetic electron transport and proton flux under moderate heat stress, Photosynth. Res. 100 (2009) 29–43.
[26] F. Perreault, N.A. Ali, C. Saison, R. Popovic, P. Juneau, Dichromate effect on energy dissipation of photosystem II and photosystem I in *Chlamydomonas reinhardtii*, J. Photochem. Photobiol. B: Biol. 96 (2009) 24–29.
[27] R.E. Coopman, F.P. Fuentes-Neira, V.F. Briceño, H.M. Cabrera, L.J. Corcuera, L.A. Bravo, Light energy partitioning in photosystems I and II during development of *Nothofagus nitida* growing under different light environments in the Chilean evergreen temperate rain forest, Trees Struct. Funct. 24 (2010) 247–259.
[28] S.Z. Wang, F.L. Chen, S.Y. Mu, D.Y. Zhang, X.L. Pan, D.J. Lee, Simultaneous analysis of photosystem responses of *Microcystis aeruginoga* under chromium stress, Ecotoxicol. Environ. Saf. 88 (2012) 163–168.
[29] S.Z. Wang, D.Y. Zhang, X.L. Pan, Effects of cadmium on the activities of photosystems of Chlorella pyrenoidosa and the protective role of cyclic electron flow, Chemosphere <http://dx.doi.org/10.1016/j.chemosphere.2013.04.070>.
[30] X.L. Pan, D.Y. Zhang, X. Chen, A.M. Bao, L.H. Li, Antimony accumulation, growth performance, antioxidant defense system and photosynthesis of Zea mays in response to antimony pollution in soil, Water Air Soil Pollut. 215 (2011) 517–523.
[31] H.K. Lichtenthaler, A.R. Wellburn, Determination of total carotenoids and chlorophyll *a* and *b* of leaf extracts in different solvents, Biochem. Soc. Trans. 603 (1983) 591–592.
[32] E. Pfündel, C. Klughammer, U. Schreiber, Monitoring the effects of reduced PS II antenna size on quantum yields of photosystems I and II using the Dual-PAM-100 measuring system, PAM Appl. Notes 1 (2008) 21–24.
[33] C. Klughammer, U. Schreiber, Complementary PS II quantum yields calculated from simple fluorescence parameters measured by PAM fluorometry and the Saturation Pulse method, PAM Appl. Notes 1 (2008) 27–35.
[34] D.M. Kramer, G. Johnson, O. Kiirats, G.E. Edwards, New fluorescence parameters for the determination of Q_A redox state and excitation energy fluxes, Photosynth. Res. 79 (2004) 209–218.
[35] K. Suzuki, Y. Ohmori, E. Ratel, High root temperature blocks both linear and cyclic electron transport in the dark during chilling of the leaves of rice seedlings, Plant Cell Physiol. 52 (2011) 1697–1707.
[36] T. Platt, C.L. Gallegos, W.G. Harrison, Photoinhibition of photosynthesis in natural assemblages of marine phytoplankton, J. Mar. Res. 38 (1980) 687–701.
[37] S. Saroussi, S. Beer, Alpha and quantum yield of aquatic plants derived from PAM fluorometry: uses and misuses, Aquat. Bot. 86 (2007) 89–92.
[38] D.A. Kramer, C.A. Sacksteder, A diffused-optics flash kinetic spectrophotometer (DOFS) for measurements of absorbance changes in intact plants in the steady-state, Photosynth. Res. 56 (1998) 103–112.
[39] S.R. Chakilam, Metal effects on carotenoid content of cyanobacteria, Int. J. Bot. 8 (4) (2012) 192–197.
[40] G.Y. Huang, Y.S. Wang, Physiological and biochemical responses in the leaves of two mangrove plant seedlings (*Kandelia candel* and *Bruguiera gynmorrhiza*) exposed to multiple heavy metals, J. Hazard. Mater. 182 (2010) 848–854.
[41] M. Gupta, P. Chandra, Bioaccumulation and toxicity of mercury in rooted-submerged macrophyte *Vallisneria spiralis*, Environ. Pollut. 103 (1998) 327–332.
[42] D.D.K. Prasad, A.R.K. Prasad, Effect of lead and mercury on chloropyll synthesis in mung bean seedlings, Phytochemistry 26 (4) (1987) 881–883.
[43] Y. Horie, H. Ito, M. Kusaba, A. Tanaka, Participation of chlorophyll *b* reductase in the initial step of the degradation of light-harvesting chlorophyll a/b-protein complexes in Arabidopsis, J. Biol. Chem. 284 (26) (2009) 17449–17456.
[44] M.K. Chettri, C.M. Cook, E. Vardaka, T. Sawidis, T. Lanaras, The effects of Cu, Zn and Pb on the chlorophyll content of the lichens *Cladonia convoluta* and *Cladonia rangiformis*, Environ. Exp. Bot. 39 (1998) 1–10.
[45] M. Bačkor, J. Zetikova, Effects of copper, cobalt and mercury on the chlorophyll content of lichens *Cetraria islandica* and *Flavocetraria cucullata*, J. Hattori. Bot. Lab. 93 (2003) 175–187.
[46] M. Bačkor, A. Dzubaj, Short-term and chronic effects of copper, zinc and mercury on the chlorophyll content of four lichen photobionts and related alga, J. Hattori. Bot. Lab. 95 (2004) 271–284.
[47] K. Dankov, M. Busheva, D. Stefanov, E.L. Apostolova, Relationship between the degree of carotenoid depletion and function of the photosynthetic apparatus, J. Photochem. Photobiol. B: Biol. 96 (2009) 49–56.
[48] A.J. Young, The photoprotective role of carotenoids in higher plants, Physiol. Plant 83 (1991) 702–708.
[49] M. Bernier, R. Popovic, R. Carpentier, Mercury inhibition at the donor side of photosystem II is reversed by chloride, FEBS Lett. 321 (1993) 19–23.
[50] C. Pagliano, M. Raviolo, F.D. Vecchia, R. Gabbrielli, C. Gonnelli, N. Rascio, R. Barbato, N. La Rocca, Evidence for PSII donor-side damage and photoinhibition induced by cadmium treatment on rice (*Oryza Sativa* L.), Photochem. Photobiol. B: Biol. 84 (2006) 70–78.
[51] C.M. Lu, C.W. Chau, J.H. Zhang, Acute toxicity of excess mercury on the photosynthetic performance of cyanobacterium, *S. platensis*-assessment by chlorophyll fluorescence analysis, Chemosphere 41 (2000) 191–196.
[52] F. Van Assche, H. Clijsters, Effect of metals on enzyme activity in plants, Plant Cell Environ. 13 (1990) 195–206.
[53] J.L. Hall, Cellular mechanisms for heavy metal detoxification and tolerance, J. Exp. Bot. 53 (2002) 1–11.
[54] A.K. Matoo, J.B. Marder, M. Edelman, Dynamics of the photosystem II reaction center, Cell 56 (1989) 241–246.
[55] H. Jiang, B. Qiu, Inhibition of photosynthesis by UV-B exposure and its repair in the bloom-forming cyanobacterium *Microcystis aeruginosa*, J. Appl. Phycol. 23 (2011) 691–696.
[56] S. Bailey, A. Melis, K.R.M. Mackey, P. Cardol, G. Finazzi, G. van Dijken, G.M. Berg, K. Arrigo, J. Shrager, A. Grossman, Alternative photosynthetic electron flow to oxygen in marine *Synechococcus*, Biochim. Biophys. Acta 1777 (2008) 269–276.
[57] W. Huang, S.B. Zhang, K.F. Cao, Stimulation of cyclic electron flow during recovery after chilling-induced photoinhibition of PSII, Plant Cell Physiol. 51 (2010) 1922–1928.
[58] S. White, A. Anandraj, F. Bux, PAM fluorometry as a tool to assess microalgal nutrient stress and monitor cellular neutral lipids, Bioresour. Technol. 102 (2011) 1675–1682.
[59] B. Wodala, G. Eitel, T.N. Gyula, A. őrdöG, F. Horváth, Monitoring moderate Cu and Cd toxicity by chlorophyll fluorescence and P_{700} absorbance in pea leaves, Photosynthetica 50 (2012) 380–386.
[60] M.P. Johnson, A. Zia, A.V. Ruban, Elevated ΔpH restores rapidly reversible photoprotective energy dissipation in Arabidopsis chloroplasts deficient in lutein and xanthophyll cycle activity, Planta 235 (2012) 193–204.
[61] J. Dzbek, B. Korzeniewski, Control over the contribution of the mitochondrial membrane potential ($\Delta\psi$) and proton gradient (ΔpH) to the proton motive force (Δp), J. Biol. Chem. 238 (48) (2008) 33232–33239.
[62] S. Mou, X. Zhang, N. Ye, J. Miao, S. Cao, D. Xu, X. Fan, M. An, Analysisi of ΔpH and the xanthophyll cycle in NPQ of the Antarctic sea ice alga *Chlamydomonas* sp. ICE-L, Extremophiles 17 (2013) 477–484.
[63] A. Kanazawa, D.M. Kramer, In vivo modulation of nonphotochemical exciton quenching (NPQ) by regulation of the chloroplast ATP synthase, PNAS 99 (2002) 12789–12794.
[64] W. Bilger, U. Schreiber, Chlorophyll luminescence as an indicator of stress-induced damage to the photosynthetic apparatus. Effects of heat-stress in isolated chloroplasts, Photosynth. Res. 25 (1990) 161–171.
[65] Q.X. Tang, J.M. Wei, Contribution of ΔpH and ΔE to photosynthesis of *Chlamydomonas reinhardtii*, Photosynthetica 39 (1) (2001) 127–129.